Vesicle−Micelle Transition and the Stability of the Vesicle Dispersion in Mixtures of Tetradecyldimethylamine Oxide Hemihydrochloride and Sodium Naphthalenesulfonate

Hideya Kawasaki,*,† Ryota Imahayashi,† Shimon Tanaka,† Mats Almgren,‡ Göran Karlsson,‡ and Hiroshi Maeda†

Department of Chemistry, Faculty of Science, Kyushu University 33, Hakozaki, Higashi-ku, Fukuoka 812-8581, Japan, and Department of Physical Chemistry, Uppsala University, Uppsala SE-751 21, Sweden

Received: January 22, 2003; In Final Form: April 16, 2003

Spontaneous vesicle formation was found to occur on simple mixing of two solutions: a micellar solution of tetradecyldimethylamine oxide hemihydrochloride (C14DMAO·$^1/_2$HCl) and a sodium 2-naphthalenesulfonate (NaNphS) salt solution. The stability of the vesicle dispersion and the sign of the vesicle charge depended on the mixing mole ratio β (=[NaNphS]/[C14DMAO·$^1/_2$HCl]) at 25 °C: elongated micelles ($\beta < 0.25$) → positively charged unilamellar vesicle dispersion ($0.3 < \beta < 0.5$) → sediments consisting of aggregated multilamellar vesicles ($0.55 < \beta < 0.75$) → negatively charged unilamellar vesicle dispersion ($0.75 < \beta < 5$). The β-dependent aggregation behavior of the vesicles correlated well with the change in the ζ potential of the vesicles, and it was described by the normal DLVO theory. This indicates that the repulsive double-layer force is a major factor in stabilizing the vesicle dispersion, while the main driving force of the aggregation is an attractive van der Waals force between the vesicle bilayers. CryoTEM pictures demonstrated that the vesicles showed a drastic change in microstructure upon aggregation. In the aggregated multilamellar vesicles, the electrostatic repulsion between the bilayers is suppressed by the complete binding of counterions $NphS^-$, leading to the change from unilamellar vesicles to aggregated multilamellar vesicles. It is suggested that vesicle formation in the C14DMAO·$^1/_2$HCl−NaNphS system can be attributed to the combined effect of the hydrogen bonding between the cationic and the nonionic headgroups ($-N^+-OH\cdots O-N-$) and the strong counterion $NphS^-$ binding.

Introduction

Amphiphilic molecules such as surfactants spontaneously self-assemble to a variety of aggregate structures.[1] In cationic surfactant/aromatic counterion systems, rodlike micelles can grow to form extremely long wormlike micelles due to the strong binding of aromatic counterions to the micelles, such as sodium salicylate (SS),[2−4] 3,5-dichlorobenzoate,[5] *p*-toluenesulfonate,[6] alkyl sulfonate,[7,8] and sodium naphthalenesulfonate.[9] One of the most extensively studied systems of this kind is the mixture of cetyltrimethylammonium bromide (C16TAB) with sodium salicylate (SS).[2−4] In equimolar solutions of the surfactant and counterion at concentrations as low as 10^{-3} M, the system forms long wormlike micelles, which behave like living polymers with continuous breaking and reformation of the micelles.[10] For the mixture of C16TAB with sodium 3-hydroxynaphthalene-2-carboxylate (SHNC),[11−14] continuous addition of SHNC gave the following transitions: I → N → lamellar aggregates containing the vesicles (1:1 mixture of C16TAB with SHNC) → N → I.[11,14] Here a highly viscoelastic optically isotropic liquid is denoted as I, and N is the liquid crystalline nematic phase. Cetyltrimethylammonium hydroxynaphthalenecarboxylate (C16TAHNC), obtained from an equimolar mixture of C16TAB with SHNC, formed vesicles at room temperature at concentrations less than 60 mM and the lamellar liquid crystalline phase above 60 mM. A temperature-induced micelle−vesicle transition was observed for C16TAHNC.[12−14] Sodium naphthalenesulfonate (NaNphS) is another large aromatic counterion with a naphthalene ring, which is expected to have similar hydrophobicity to that of SHNC. Contrary to the case of SHNC, the addition of NaNphS does not produce vesicles, however. The equimolar mixtures of C16TAB with NaNphS exhibited wormlike micelles at 25 °C.[9] The reason that vesicles are not formed for the C16TAB/SNphS system is still unclear, and hence, it is not always the case that addition of large aromatic counterions induces the vesicle formation.

Alkyldimethylamine oxides (C*n*DMAOs) exist as either nonionic [$C_nH_{2n+1}(CH_3)_2N\rightarrow O$] or cationic (protonated) species [$C_nH_{2n+1}(CH_3)_2N^+-OH$]. The relative population of the two components (i.e. the degree of protonation α) depends on the pH of the solution. Evidence for a short-range attractive interaction between the nonionic and the cationic headgroups has been suggested in the solid state,[15,16] in the micelles in solution,[17,18] and in adsorbed films at the solid−solution interface.[19,20] Reversible vesicle formation from threadlike micelles was observed to occur in oleyldimethylamine oxide aqueous solutions by changing pH.[21] The short-range attractive interaction has been suggested to be a hydrogen bond between the nonionic and the cationic headgroups.[22−25] Support for the proposed hydrogen bond has been found from infrared spectroscopy.[26]

Recently, we reported the phase behavior of fully ionized tetradecyldimethylhydroxylammonium chloride

* Corresponding author. Telephone: 81-92-642-4367. Fax: 81-92-642-2607. E-mail: hkawascc@mbox.nc.kyushu-u.ac.jp.
† Kyushu University.
‡ Uppsala University.

10.1021/jp0300804 CCC: $25.00
Published on Web 07/19/2003

(C14DMAO·HCl) (i.e. $\alpha = 1$) in the presence of sodium 2-naphthalenesulfonate (NaNphS).[27] In the equimolar mixture of C14DMAOH·Cl with NaNphS, a solid crystalline phase was observed below 54 °C and a lamellar liquid crystalline phase above 54 °C at a surfactant concentration of 20 mM, in contrast to the long wormlike micelles of many other cationic micelle−aromatic counterion pairs such as C16TAB−NaNphS.[9] Vesicle dispersion was not observed for the C14DMAO·HCl−NaNphS system even after dilution to 1 mM. The high value of the surfactant packing parameter ($p \sim 1$) of the $C14DMAOH^+NphS^-$ system was suggested to originate from the hydrogen bonding between the two neighboring cationic headgroups[18,25] plus the suppressed charge repulsion by counterion binding.

In this article, we report on the phase behavior of a mixed surfactant system of tetradecyldimethylamine oxide hemihydrochloride C14DMAO·$^1/_2$HCl (i.e. $\alpha = 0.5$) in the presence of NaNphS. We find that addition of NaNphS to micellar solutions of C14DMAO·$^1/_2$HCl produced vesicles spontaneously, in contrast with the case of the full-ionized C14DMAO·HCl−NaNphS system.[27] To understand the aggregation behavior of the vesicles, the electrophoretic mobilities of the vesicles and the chloride ion activity were measured. The aggregation behavior of the vesicles was analyzed on the basis of the DLVO theory. The microstructures of vesicules were directly observed by cryoTEM.

Materials and Methods

Materials. Water was prepared by distillation and then passage through an ultrapure water system consisting of an ion exchange, activated carbon cartridge and a 0.2 μm filter (Branstead Co). The resulting water had a conductivity of 18 MΩ cm^{-1} at 25 °C. Tetradecyldimethylamine oxide (C14DMAO) (GERBU CO.) was recrystallized three times from hot acetone. After recrystallization, there was a single peak in chromatograms of high performance liquid chromatography (HPLC) (TOSOH Co., Japan) with an ODS-120T column (MeOH/H_2O = $^7/_3$). The nonionic C14DMAO sample was dissolved in water, and hydrochloric acid was added to protonate just half of the amine oxide. The solution thus prepared was freeze-dried, and we obtained the half-ionized solid sample (C14DMAO·$^1/_2$HCl). Sodium 2-naphthalenesulfonate (NaNphS), sodium benzenesulfonate (NaBzS), and Na_2SO_4 were purchased from Tokyo Kasei Kogyo and used without further purification. Tetradecyltrimethylammonium chloride (C14TA) (NACALAI TESQUE CO.) was recrystallized two times from hot acetone.

Turbidity. Turbidity measurements were performed at 25 °C with a Jasco Ubest-50 UV/vis spectrophotometer, equipped with a thermostat cell holder and a magnetic stirring device, using quartz cells of 1 cm path length. Turbidity expressed in transmittance was measured at 400 nm.

Viscosity. The specific viscosity was measured at 25 ± 0.02 °C using an Ostwald viscometer (flow time of water: 91.7 ± 0.1 s).

Dye Solubilization. The saturated solubilization of a water-insoluble dye, Sudan III, by the micelles or vesicles was examined for aqueous solutions of C14DMAO·$^1/_2$HCl in the presence of NaNphS at 25 ± 1 °C. After removal of excess undissolved dye by a Millipore filter of 0.2 μm, the absorbance of the solubilized dye in the solutions was measured with a Jasco Ubest-50 UV/vis spectrophotometer at 500 nm.

Differential Scanning Calorimetry (DSC). The dissolution temperature of the hydrated crystalline solids in the presence of water was determined from the maximum temperature of the endothermic peak with a Seiko Instrument DSC 120 at a heating rate of 1 °C/min.

Cryo-Transmission Electron Microscopy (cryoTEM). The electron microscopy investigations were performed with a Zeiss 902 A instrument, operating at 80 kV. Specimens were prepared by a blotting procedure, performed in a chamber with controlled temperature and humidity. A drop of the sample solution was placed onto an EM grid coated with a perforated polymer film. Excess solution was then removed with a filter paper, leaving a thin film of the solution on the EM grid. Vitrification of the thin film was achieved by rapid plunging of the grid into liquid ethane held at its freezing point. The vitrified specimen was then transferred in the cold state to the microscope and investigated at 108 K.

Polarizing Microscopy. The presence of multilamellar structures was revealed by examination in a Nikon polarization microscope E 600 POL, equipped with a LINKAM LTS-E 350 hot stage.

Chloride Ion Activity. The Cl^- ion activity was obtained from emf data measured with a Digital Electrometer/R8240 (ADVNTEST) using Ag/AgCl electrodes which were made by electroplating a silver wire (2 mm diameter) in 0.1 M NaCl solution. The activity of the Cl^- ion, a_{Cl}, of NaCl for the calibration was obtained before the measurement of the sample solutions, and the plot of log a_{Cl} versus emf showed a good linearity: 55.2 ± 0.1 mV for Δ log a_{Cl} =1.

Electrophoretic Light Scattering (ELS). Measurements of electrophoretic mobility were carried out for the C14DMAO·$^1/_2$HCl solutions at 25 °C at different β values, using a Photal ELS-8000 electrophoretic light scattering apparatus with a He−Ne laser of 633 nm wavelength as light source (Otsuka Electronics Co). The values of E were changed ($5 < E < 30$ V cm^{-1}) in a linear region at a scattering angle of 20°. The surfactant concentration of C14DMAO·$^1/_2$HCl was fixed at 20 mM. Sample solutions were introduced into the cell by a peristaltic pump, after being filtered with a Millipore membrane (pore size 0.2 μm) three times. The measurements were usually repeated at least three times, and the average values were reported. In the case of vesicles, the measured mobilities, U, were converted to ζ potentials using the Helmholtz−Smoluchowski equation, since $\kappa R \gg 1$. Here κ is the inverse Debye screening length and R is the radius of the vesicles. The experimental procedure has been reported in detail in the literature.[28]

Dynamic Light Scattering (DLS). The average size of the vesicles was measured by an ELS-8000 (Ootsuka Electronics Co) with a He−Ne laser of 633 nm wavelength as light source using a square cell for the dynamic light scattering mode. Sample solutions were introduced into the cell after being filtered through a Millipore membrane (pore size 0.2 μm and 0.45 μm) three times. The time-dependent autocorrelation function of the scattered light intensity was measured at a scattering angle of 90° 1 week after the filtration of the solutions. The average vesicle diameters were obtained with the method of cumulants. The DLS measurements were usually repeated at least three times, and the average values were reported.

Composition of the Sediment from the Mixture of C14DMAO·$^1/_2$HCl−NaNphS. The aqueous mixtures of C14DMAO·$^1/_2$HCl−NaNphS at different mole ratios β (=NaNphS/C14DMAO·$^1/_2$HCl) (β = 0.6, 0.65, 0.7, and 0.75) were maintained at 25 °C for 1 week, resulting in sedimentation. The sediment was separated by filtration. The NaNphS content of the bulk solution in equilibrium with the sediment was determined from the UV absorption of NaNphS at λ = 320

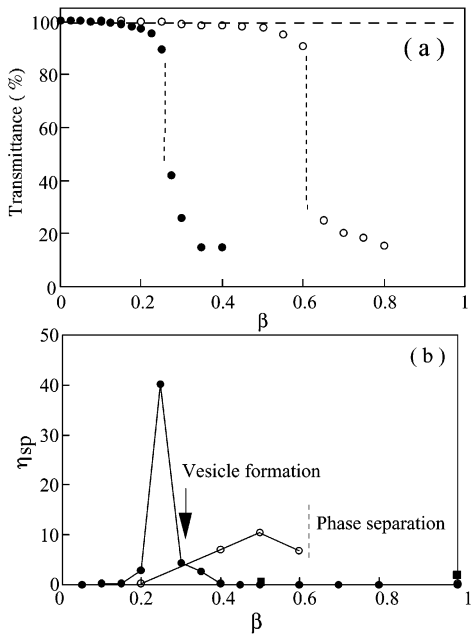

Figure 1. (a) Turbidity (expressed as transmittance at 400 nm) at 25 °C as a function of the molar ratios β [=X/C14DMAO·$^1/_2$HCl] (X = NaNphS, NaBzS, and Na_2SO_4): closed circles, NaNphS; open circles, NaBzS; broken line, Na_2SO_4. The surfactant concentration is fixed to be 20 mM. (b) Specific viscosity ($\eta_{sp} = \eta/\eta_0 - 1$) of the C14DMAO·$^1/_2$HCl aqueous solution (20 mM) at 25 °C as a function of the mole ratio of β (=X/C14DMAO·$^1/_2$HCl) (X = NaNphS, NaBzS, and Na_2SO_4), where η and η_0 are the viscosity of the solution and water, respectively: ●, NaNphS; ○, NaBzS; ■, Na_2SO_4.

nm. From the NaNphS content of the total system and that of the bulk solution, we determined the composition of the sediment.

Results and Discussion

Turbidity and Viscosity. Figure 1 shows a plot of (a) the turbidity and (b) the specific viscosity of C14DMAO·$^1/_2$HCl aqueous solutions (a fixed surfactant concentration, 20 mM) as a function of the mole ratio of β (=X/[C14DMAO·$^1/_2$HCl]) (X = NaNphS, NaBzS, and Na_2SO_4). In the case of NaNphS, the solutions were transparent up to $\beta \sim 0.25$ and they are in a single micellar phase region. Close to $\beta = 0.25$, the viscosity increases sharply, as shown in Figure 1b. The solution becomes viscoelastic, suggesting the formation of elongated micelles around $\beta \sim 0.25$. The maximum specific viscosity is around 40, which is higher than the maximum viscosity reported for the fully ionized C14DMAO·HCl/NaNphS system (∼20),[27] indicating more pronounced micellar growth in the case of C14DMAO·$^1/_2$HCl. This is consistent with the pronounced micelle growth observed for C14DMAO·$^1/_2$HCl solutions in 0.1 M NaCl without NaNphS.[17] At $\beta = 0.3$, the solution becomes slightly turbid and the viscosity decreases remarkably, indicating the structural change of the micelles. By cryoTEM observation we found that the structural changes at $\beta = 0.3$ corresponded to the transition from elongated micelles to vesicles. A liquid−liquid phase separation was observed at $\beta = 0.27$. The top solution was turbid due to the existence of vesicles, while the bottom solution was clear and viscoelastic, probably containing long micelles. Further addition of NaNphS produced sediments in the β range ($0.55 < \beta < 0.75$). Above $\beta > 0.75$, however, the sediment dispersed to form a vesicle dispersion again. Even at $\beta = 5$, a stable vesicle dispersion was observed with no indication of sedimentation for at least 2 months. These results indicate that a micelle−vesicle transition occurs on addition of NaNphS, in contrast to the case of the system of fully ionized C14DMAO·HCl−NaNphS at 25 °C, in which solid crystals were formed for $\beta > 0.5$, with a wide region of β ($0.5 < \beta < 1$) for the coexistence of micelles and solid crystals.[27]

In the case of NaBzS, all samples are micellar solutions up to $\beta = 0.6$. Above $\beta \sim 0.2$, the viscosity increases gradually, indicating formation of elongated micelles, as shown in Figure 1b. The maximum viscosity is larger for NaNphS than for NaBzS (the maximum specific viscosity ∼ 40 for NaNphS and ∼10 for NaBzS), indicating a more pronounced micellar growth in the case of NaNphS. This is expected from the increased hydrophobicity due to the naphthalene ring of NaNphS.[27] Above $\beta \sim 0.6$, liquid−liquid phase separation occurred. Both the top and the bottom solution were isotropic clear solutions capable of solubilizing a water insoluble dye, Sudan III. We could not detect any vesicle formation for the solutions by interference contrast microscopy. Na_2SO_4 was found to be ineffective to induce a structural change of the micelle, despite its content of divalent anions.

Dye Solubilization. Figure 2a shows a plot of the absorbance of Sudan III in the C14DMAO·$^1/_2$HCl aqueous solution (20 mM) as a function of the mole ratio β (=[NaNphS]/[C14DMAO·$^1/_2$HCl]). The absorbance of Sudan III in the range from 0.6 to 1.2 is due to the solubilization of the dye by the micelles or the vesicles. In the range $\beta = 0.6-0.7$, sediments appeared and there was no solubilization in the solution part. However, we found that the dye was solubilized by the sediment, which can be easily recognized by the direct observation of the red colored sediment (Figure 2b). This indicates that the sediment is not a crystalline solid but comprises liquidlike hydrocarbon chains at 25 °C. From a clear endothermic peak in the DSC curve for the C14DMAO·$^1/_2$HCl−NaNphS solutions (not shown), it was found that the melting temperature of the hydrocarbon chains was 21 °C, irrespective of the β values ($0.5 < \beta < 1$). At temperatures lower than 21 ° C, the crystalline solids were formed in this β range and there was no solubilization of the dye. The dye solubilization experiment, thus, gives a simple indication of the liquidlike nature of the hydrocarbon chains in the aggregates.

CryoTEM Observation of the Vesicles in the System of C14DMAO·$^1/_2$HCl−NaNphS. CryoTEM pictures of the vesicles for $\beta = 0.4$ and 1.0 in the system of C14DMAO·$^1/_2$HCl−NaNphS are shown in Figure 3 a and b, respectively. The cryoTEM micrographs give similar structures for $\beta = 0.4$ and 1.0. The vesicles are polydisperse, from small to very large. Their diameters are from 30 nm up to 500 nm and larger. The vesicles contain mainly unilamellar vesicles (Figure 3a and b), but in addition some multilamellar vesicles (Figure 3c). It seems that the distance between the bilayers in a multilamellar vesicle ranges from 20 to 30 nm. For the vesicles at $\beta = 0.4$, we can also see that the bilayers are often irregular and have openings. From DLS measurement, the average diameters of the vesicles were 135 ± 59 nm at $\beta = 0.4$ and 186 ± 91 nm at $\beta = 1.0$. The polydispersity obtained from the cumulant analysis is a measure of the size distribution, and a narrow size distribution is suggested if it is below 0.1.[29] The polydispersity for the vesicles was estimated to be 0.18 for $\beta = 0.4$ and 0.24 for $\beta = 1.0$, suggesting a broad size distribution of the vesicles, consistent with the cryoTEM observation.

The cryoTEM micrograph of the sediment at $\beta = 0.6$ is shown in Figure 4 a. The sediment consists of many aggregated vesicles, which have diameters from 50 nm up to 500 nm or larger. We can also see larger bilayer structures (not shown),

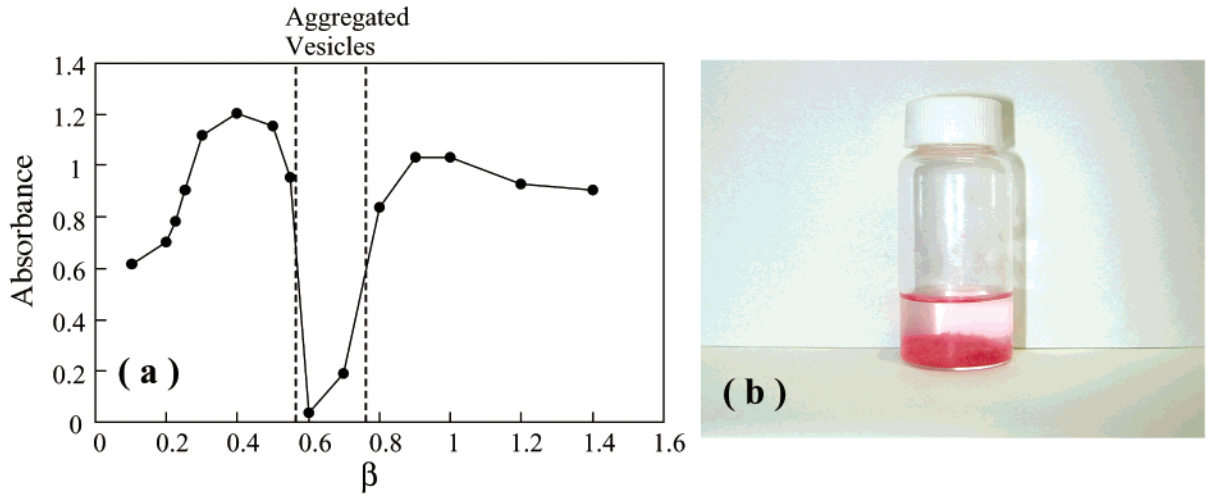

Figure 2. (a) Absorbance of Sudan III in C14DMAO·$^1/_2$HCl solutions at 25 °C as a function of the molar ratio β (=NaNphS/C14DAO·$^1/_2$HCl). The surfactant concentration is 20 mM. (b) Sediments ($\beta = 0.6$) solublize a water insoluble dye, Sudan III.

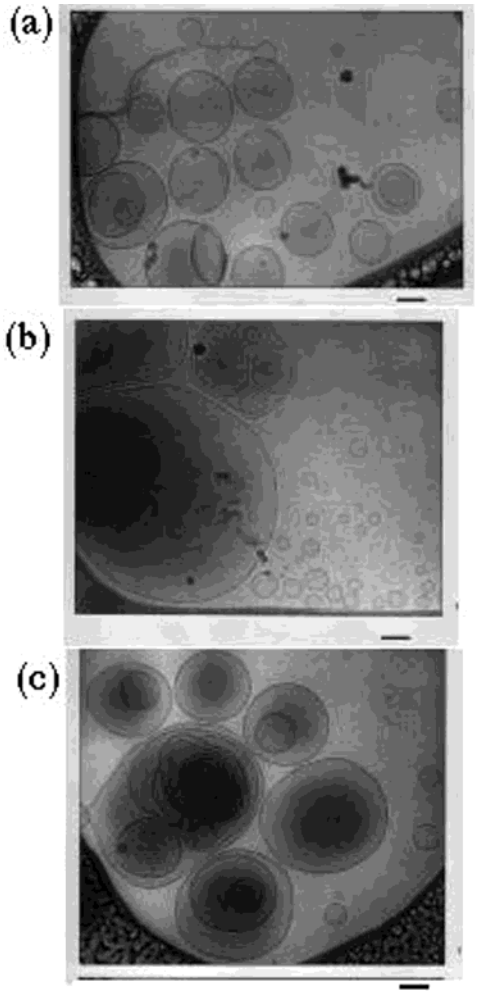

Figure 3. (a) Cryoscopic transmission electron micrographs of C14DMAO·$^1/_2$HCl solutions of 20 mM in the presence of NaNphS at 25 °C: (a) $\beta = 0.4$; (b) $\beta = 1.0$; (c) $\beta = 0.4$. The bar in the figure corresponds to 100 nm.

in addition to clusters of multilamellar vesicles. Polarizing microscopy observation of the sediment confirmed the presence of Maltese crosses that are characteristic for large spherical multilamellar structures (Figure 4b). For the solutions containing vesicles at $\beta = 0.4$ and 1.0, on the other hand, the polarizing microscopy observation did not show the Maltese crosses, and hence, these solutions were isotropic.

It should be emphasized that the mulitilamellar vesicles showed a drastic change in microstructure upon aggregation. The aggregated multilamellar vesicles have thick outer-shell structures with the total thickness of typically about 40 nm, as shown in Figure 4a. The shell structures comprised closely stacked bilayers. It appears that the spacing between the closely stacked bilayers is much less than 10 nm, much smaller than that of the dispersed multilamellar vesicles ($\beta = 0.4$ and 1.0). In the aggregated vesicles, the electrostatic repulsion between the bilayers is expected to be suppressed by the counterion $NphS^-$ binding, resulting in the change from unilamellar vesicles to aggregated multilamellar vesicles. The reduction of the bilayer distance in aggregated vesicles has also been reported for the system of C16TAB/SHNC on the basis of freeze−fracture electron microscopy (FF-TEM).[14]

The sedimentation of the multilamellar vesicles means that the closely stacked bilayers should have a density higher than that of water. Such sediments of multilamellar vesicles with a density higher than that of water have recently been reported for vesicles from ethylene oxide/butylene oxide diblock copolymers.[30]

Electrophoretic Mobilities of the Vesicles in the System of C14DMAO·$^1/_2$HCl−NaNphS and the Chloride Ion Activity. The addition of NaNphS to a C14DMAO·$^1/_2$HCl solution (20 mM) produced the following sequence:

elongated micelles ($\beta < 0.25$) → 2 phase ($\beta \sim 0.25$) →
vesicles dispersion ($0.3 < \beta < 0.55$) →
aggregated vesicles ($0.55 < \beta < 0.75$) →
vesicles dispersion ($0.75 < \beta < 5$)

This strongly suggests a change in the surface charge type of the vesicles by addition of NaNphS. To clarify the surface charge of the vesicles, we measured the electrophoretic mobility of the vesicles as a function of β, together with the Cl^- ion activity, a_{Cl}. Figure 5 shows (a) the electrophoretic mobility U and (b) the Cl^- ion activity a_{Cl} as a function of β for C14DMAO·$^1/_2$HCl solutions with NaNphS. The ζ potentials of the vesicles are also given in Figure 5. In C14DMAO·$^1/_2$HCl solution (i.e. $\beta = 0$), a_{Cl} is 5.2 mM, which corresponds to a degree of Cl^- counterion binding to the micelles of 0.48. The Cl^- ion activity increases with β linearly, indicating that the Cl^- ions are displaced from the micelles by the added $NphS^-$ anion. The decrease of the positive U values in the micellar solutions ($\beta < 0.25$) may be explained by the decrease of the

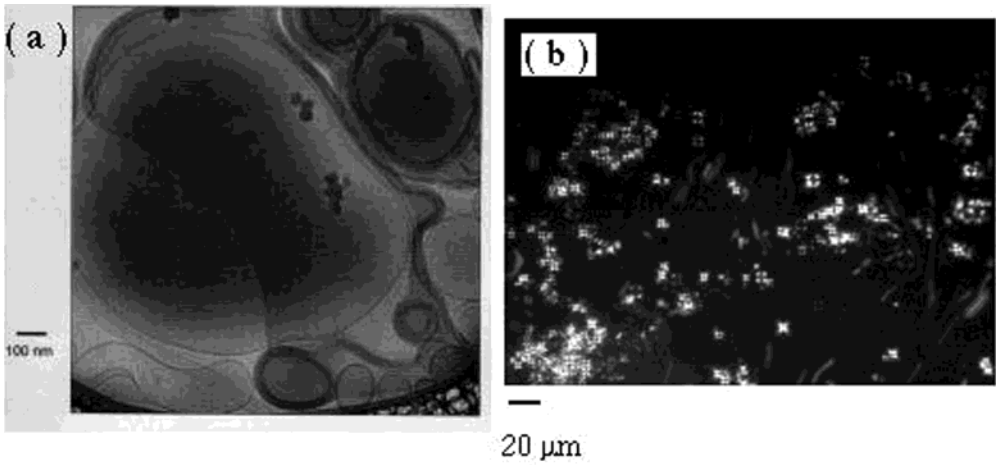

Figure 4. (a) Cryoscopic transmission electron micrographs of C14DMAO·$^1/_2$HCl solutions of 20 mM in the presence of NaNphS of $\beta = 0.6$ at 25 °C. The bar in the figure corresponds to 100 nm. (b) Polarization micrograph of the sediment in C14DMAO·$^1/_2$HCl solutions of 20 mM in the presence of NaNphS of $\beta = 0.6$ at 25 °C. The bar in the figure corresponds to 20 μm.

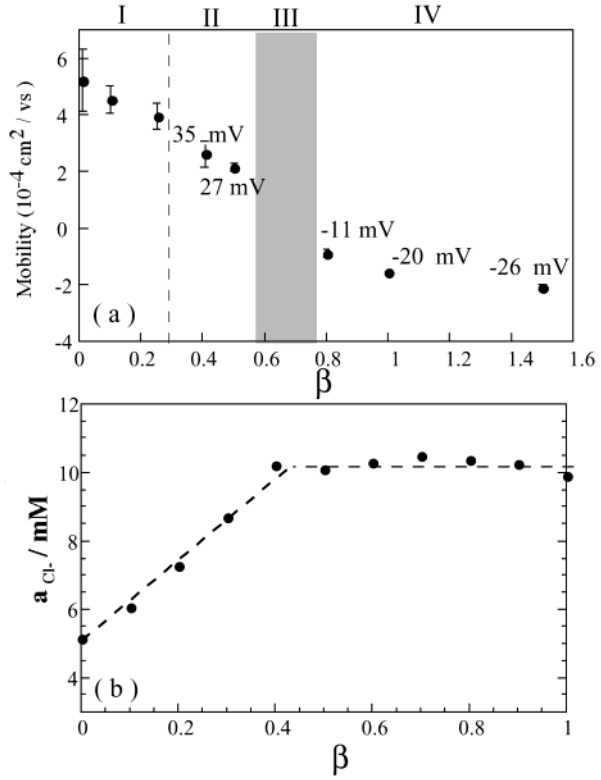

Figure 5. β dependence of the electrophoretic mobilities for the elongated micelles and the vesicles of C14DMAO·$^1/_2$HCl in the presence of NaNphS at 25 °C, together with the measured Cl^- ion activity, a_{Cl}. The surfactant concentration is 20 mM: I, rodlike or threadlike micelles; II, positively charged vesicles; III, aggregated vesicles; IV, negatively charged vesicles.

micelle charge due to the strong counterion $NphS^-$ binding to the micelle surface. By reduction in the electrostatic interaction between the headgroups, the formation of elongated micelles is favorable in the β range less than 0.25. In vesicular solutions ($\beta > 0.4$), the Cl^- ion activities were almost constant irrespective of β and are nearly equal to the total Cl^- ion concentration of the system (i.e. $a_{Cl} \sim 10$ mM). This indicates that the Cl^- ions are completely displaced from the vesicles by the added $NphS^-$ anion or there is no binding of Cl^- ion to the vesicles. We found that charge reversal of the vesicles from positive to negative occurred in the β range ($0.6 < \beta < 0.7$) (Figure 5a) where the sediment of aggregated vesicles appeared. The ζ potential of the aggregated vesicles is, thus, considered to be nearly equal to zero. By further addition of NaNphS, the excess $NphS^-$ anions adsorb onto the aggregated vesicles, resulting in dispersion of negatively charged vesicles. A possible adsorption of the Cl^- anion to the electrically neutralized vesicles is ruled out, since the Cl^- ion activity was almost constant even as charge reversal of the vesicles occurred (Figure 5b).

Vesicle Interaction and Aggregation (the DLVO Theory). The electrophoretic results indicate that the stability of the vesicle dispersion correlates well with the ζ potential. Below about |10| mV it appears that the vesicle dispersion becomes unstable and vesicle aggregation occurs, as shown in Figure 5a. In this section, we consider the vesicle aggregation behavior on the basis of the DLVO theory. According to the DLVO theory, the total potential energy, $V_{tot}(d)$ of interactions between charged colloid particles is given by the sum of the energy of the repulsive interaction of the double layer, $V_R(d)$, and that of attractive interaction of the van der Waals forces, $V_A(d)$:[31]

$$V_{tot}(d) = V_R(d) + V_A(d) \tag{1}$$

where d is the interparticle separation. $V_R(d)$ may be expressed by[32−34]

$$V_R(d) = 2\pi\epsilon\epsilon_0 a\phi_0^2 \ln[1 + \exp(-\kappa d)] \quad \text{(constant potential)} \tag{2}$$

$$V_R(d) = -2\pi\epsilon\epsilon_0 a\phi_0^2 \ln[1 - \exp(-\kappa d)] \quad \text{(constant charge)} \tag{3}$$

where ϕ_0 is the surface potential of the vesicles. ϵ_0, ϵ, a, and $1/\kappa$ are the dielectric permittivity in a vacuum, the relative dielectric coefficient of the aqueous medium, the radius of the vesicle, and the Debye screening length, respectively.

The unilamellar vesicles may be regarded as colloidal particles with a shell of outer radius a and thickness l. According to the Vold theory, the van der Waals interaction energy of two spherical colloidal particles with the outer shell (see Figure 6) is expressed as[35,36]

$$-12V_A(d) = H_{11}(A_{11}^{1/2} - A_{22}^{1/2})^2 + H_{22}(A_{22}^{1/2} - A_{33}^{1/2})^2 + 2H_{12}(A_{11}^{1/2} - A_{22}^{1/2})(A_{22}^{1/2} - A_{33}^{1/2}) \tag{4}$$

where

$$H_{x,y} = y/(x^2 + xy + x) + y/(x^2 + xy + x + y) + 2\ln[(x^2 + xy + x)/(x^2 + xy + x + y)]$$

$$x = (d + 2l)/2(a - l), \quad y = 1 \qquad \text{for } H_{11}$$

$$x = d/2a, \quad y = 1 \qquad \text{for } H_{22}$$

$$x = (d + l)/2(a - l), \quad y = a/(a - l) \qquad \text{for } H_{12}$$

In the case of unilamellar spherical vesicles ($A_{11} = A_{33}$), the $V_A(d)$ may be expressed by[32]

$$-12V_A(d) = A_{eff}(H_{11} + H_{22} - 2H_{12}) \tag{5}$$

A_{eff} denotes the effective Hamarker constant of the vesicle bilayer in water. Here, we use the following relations,

$$\begin{aligned} A_{121} &\cong (A_{11}^{1/2} - A_{22}^{1/2})^2 \\ A_{232} &\cong (A_{22}^{1/2} - A_{33}^{1/2})^2 \\ A_{212} &\cong A_{121} \end{aligned} \tag{6}$$

Using eqs 1−6, calculations were made for $a = 75$ nm from DLS, $1/\kappa = 3.04$ nm at 10 mM NaCl, and the bilayer thickness $l = 3.6$ nm,[37] in accordance with the experimental results. It is assumed that the A_{eff} of the vesicles in the system of C14DMAO1/2HCl−NaNphS is equal to that of the bilayer of dodecyldimethylamine oxide in water (i.e. $A = 0.5 \times 10^{-20}$ J).[38]

Figure 7 shows the calculated interaction potential energy, $V_{tot}(d)$, between the two vesicles. Above $\phi_0 = 20$ mV, the maximum value of V_{tot} (i.e. the potential barrier against the aggregation of vesicles) is well above $1kT$, predicting a stable vesicle dispersion. The maximum V_{tot} decreases as ϕ_0 decreases. At $\phi_0 = 5$ mV, the maximum in the V_{tot} disappears, indicating a rapid coagulation of the vesicles. From the DLVO theory, it seems that $\phi_0 \sim 10$ mV corresponds to a borderline between aggregation and dispersion. This is consistent with the electrophoretic experiments for the vesicles: the aggregation occurred below the ζ potential of about |10| mV. The aggregation behavior of the vesicles can thus be described by the DLVO theory, indicating that repulsive double-layer forces are a major factor in stabilizing the vesicle dispersion, while the major driving force of the vesicle aggregation is an attractive interaction of the van der Waals forces between the vesicle bilayers. The vesicle dispersion of C14DMAO·$^1/_2$HCl−NaNphS stabilized by electrostatic repulsion is similar to the dispersion stability of glycolipid vesicles,[32] phospholipid vesicles,[39] and catanioinic vesicles.[40] It should be noted that the simple DLVO theory presented here, which was based only on competition between van der Waals and electrostatic interactions, is applicable strictly for colloidal particles with a homogeneous size distribution. The present system has rather high polydispersity in the size distribution, and hence the present treatment is only a rough estimation.

The polydispersity of the unilamellar vesicles in C14DMAO·$^1/_2$HCl−NaNphS system implies that the bending constant of the bilayers is small,[41] leading to the Helfrich fluctuation forces in the flexible bilayers. It has been reported that charging the bilayer results in an increase of its bending rigidity in the Debye−Huckel regime.[42] It is thus considered that the Helfrich fluctuation forces are suppressed by charging the bilayer of the vesicle. The decrease of the charge of the vesicle by adding NaNphS is expected to increase the Helfrich fluctuation force of the bilayers. Furthermore, the bound $NphS^-$ counterion could be looked on as a cosurfactant with a shorter chain length, which also leads to the reduction in its bending rigidity.[43,44] These two factors suggest the dispersing effect of the vesicle, which, however, is the opposite of the experimental result. Therefore, it is likely that the electrostatic repulsive forces are quenched by adding NaNphS more than the increase of the Helfrich interactions, leading to aggregation and multilamellar vesicles. However, it cannot be ruled out entirely that the Helfrich fluctuation forces act as an additional stabilizing force against aggregation. The Helfrich fluctuation forces may be partly responsible for the stability of the vesicle suspension against aggregation.

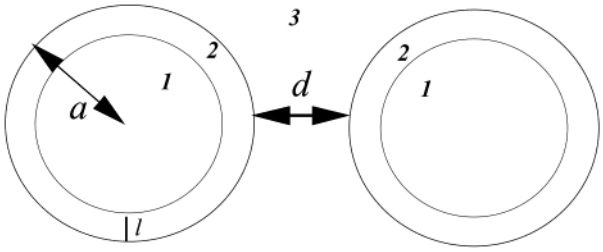

Figure 6. Schematic picture of two spherical colloidal particles with outer shell length l at a separation d. In the case of unilamellar spherical vesicles, $A_{11} = A_{33}$.

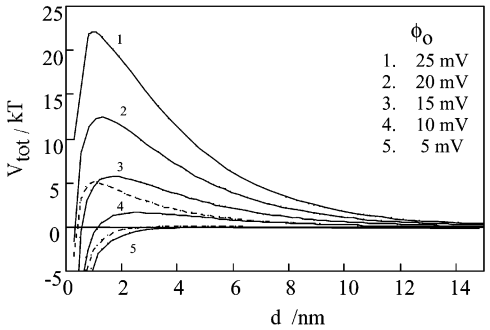

Figure 7. Total interaction potential energy, $V_{tot}(d)$, between two vesicles of radius a at 25 °C from eqs 1−4. $a = 75$ nm, $\kappa^{-1} = 3.04$ nm (10 mM NaCl), $l = 3.6$ nm, $A_{eff} = 0.5 \times 10^{-20}$ J. The surface potential ϕ_0 is given in the figure. Solid curves are $V_{tot}(d)$ under constant potential conditions. For $\phi_0 = 5$ and 10 mV, $V_{tot}(d)$ under constant charge conditions is also plotted by broken lines.

Composition of the Aggregated Vesicles. The compositions of the aggregated vesicles at 25 °C were determined at different β values ($\beta = 0.6$, 0.65 , 0.7, and 0.75). The mole ratios of the surfactant C14DMAO to the counterion $NphS^-$ in the aggregated vesicles were found to be nearly equal to 2: the ratios were 2.1, 2.1, 2.1, and 1.9 for $\beta = 0.6$, 0.65, 0.7, and 0.75, respectively. This indicates that the aggregated vesicles consist of a 1:1 complex between the nonionic and the cationic surfactant with a counterion $NphS^-$, rather than a simple $C14DMAOH^+$ $NphS^-$ salt. This assigned composition was also supported by the elementary analysis for $\beta = 0.6$ [*C%:H%:N% = 69.22:10.84:3.82 (found) and C%:H%:N% = 69.76:10.87:3.84 (calcd)*]. The specific attractive interaction between the nonionic and the cationic surfactant should exist in the vesicles. It is most likely that the hydrogen bonding between the nonionic and the cationic headgroups ($-N^+-OH\cdots O-N-$) is responsible for the 1:1 complex formation.[18,26]

Phase Behavior in an Equimolar Mixture of Nonionic C14DMAO and Cationic C14TACl in the Presence of NaNphS. To examine the role of the proposed hydrogen bonding between the cationic and the nonionic headgroups in the vesicle formation of C14DMAO·$^1/_2$HCl−NaNphS systems, we used C14TACl as the cationic surfactant, in place of C14DMAO·HCl. The phase behavior of an equimolar mixture

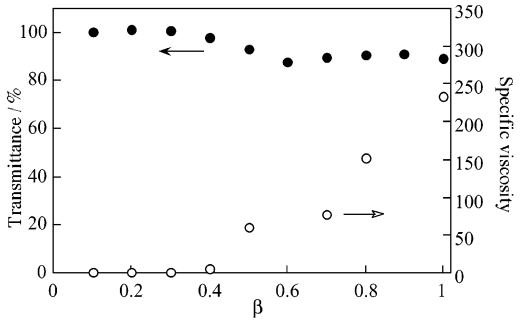

Figure 8. Turbidity (expressed as transmittance at 400 nm) and the specific viscosity ($\eta_{sp} = \eta/\eta_0 - 1$) at 25 °C as a function of the mole ratio β (=NaNphS/[C14DMAO + C14TACl]), where η and η_0 are the viscosity of the solution and water, respectively. The surfactant concentration is fixed at 20 mM. The pH of the solutions is about 9 to avoid protonation of the nonionic C14DMAO.

of cationic C14TACl and nonionic C14DMAO in the presence of NaNphS was examined. In this system, hydrogen bonding between the nonionic C14DMAO and the cationic C14TA is unlikely. Figure 8 shows the turbidity and the specific viscosity of the aqueous solutions of the equimolar mixture at 25 °C as a function of the mole ratio β (=NaNphS/[C14DMAO + C14TA]). The total surfactant concentration was fixed to be 20 mM. There is a small change in the turbidity even at $\beta \sim 1$, while the specific viscosity increases remarkably above $\beta = 0.4$, indicating a pronounced micellar growth. These turbidity and viscosity data indicate that elongated micelles are formed in the equimolar mixture of nonionic C14DMAO and cationic C14TACl on the addition of NaNphS, in contrast with the vesicle formation in the C14DMAO·$^1/_2$HCl−NaNphS system. This indicates that *the cationic C14DMAOH$^+$−nonionic C14DMAO pair* ($^1/_2 < p < 1$) has a higher packing parameter than *the cationic C14TA$^+$−nonionic C14DMAO pair* ($^1/_3 < p < {}^1/_2$). The high surfactant packing parameter of the C14DMAO·$^1/_2$HCl−NaNphS system may be attributed to the proposed hydrogen bonding of the nonionic and the cationic headgroups. The surfactant complex formed by the hydrogen bonding is considered to behave as a pseudo-double-tailed surfactant, leading to a higher packing parameter value. Hydrogen bonding is suggested to play an essential role in the vesicle formation of the C14DMAO·$^1/_2$HCl−NaNphS system, in addition to the strong binding of NaNphS to the micelle surface.

We may regard sodium naphthalenesulfonate as an anionic surfactant, and hence, this system is similar to the mixed anionic−cationic systems. It has been known that the mixed anionic−cationic systems behave as pseudo-double-tailed surfactants, leading to vesicle formation. However, we think that the mechanism of the vesicle formation of C14DMAO·$^1/_2$HCl−NaNphS differs from that of the mixed anionic−cationic systems. In the system of C14DMAO·$^1/_2$HCl−NaNphS, the pseudo-double-tailed surfactants are formed by a hydrogen bonding between the nonionic and the cationic surfactant, leading to the formation of the vesicle. The importance of the hydrogen bonding can be seen in the experimental result of no formation of the vesicles in the system of cationic C14TA$^+$−nonionic C14DMAO pairs with the counterion NphS$^-$, as mentioned above.

Conclusions

Spontaneous vesicle formation of tetradecyldimethylamine oxide hemihydrochloride (C14DMAO·$^1/_2$HCl) by the addition of sodium 2-naphthalenesulfonate (NaNphS) was found. The stability of the vesicle dispersion and the sign of the vesicle charge depended on the mole ratio β (=NaNphS/C14DMAO·$^1/_2$HCl) at 25 °C: elongated micelles ($\beta < 0.25$) → 2 phase ($\beta \sim 0.25$) → positively charged vesicle dispersion ($0.3 < \beta < 0.5$) → sediments consisting of aggregated vesicles ($0.55 < \beta < 0.75$) → negatively charged vesicle dispersion ($0.75 < \beta < 5$). Figure 9 presents a schematic picture consistent with the observed phase behavior of C14DMAO·$^1/_2$HCl−NaNphS, in addition to that of C14DMAO·$^1/_2$HCl−NaSBzS.

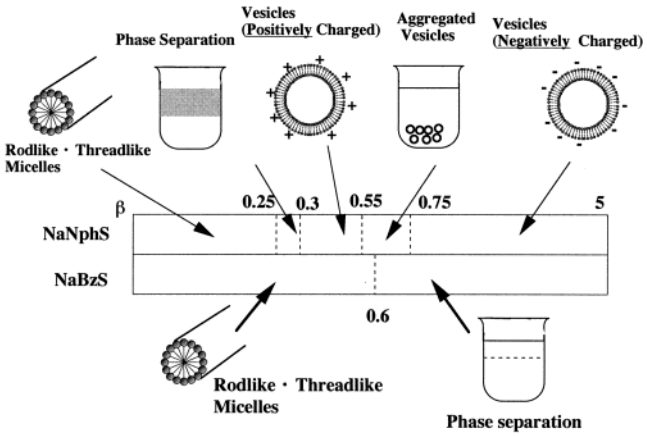

Figure 9. Schematic picture of the observed phase behavior for C14DMAO·$^1/_2$HCl − NaNphS and C14DMAO·$^1/_2$HCl − NaSBzS at 25 °C as a function of β. β = (X/C14DMAO·$^1/_2$HCl) (X = NaNphS or NaSBzS). The surfactant concentration is 20 mM.

It was found that the Cl$^-$ anions were displaced from the micelles or the vesicles by the added NphS$^-$ anions, leading to a decrease of the ζ potential of the vesicles. The ζ potential of the aggregated vesicles is considered to be nearly equal to zero. On further addition of NaNphS, the excess NphS$^-$ anion adsorbs onto the aggregated vesicles, resulting in a redispersion of negatively charged vesicles. The dispersion stability of the vesicles correlated well with the ζ potential. It seems that the borderline of the ζ potential between the coagulation and the dispersion of the vesicles is about 10 mV.

The β-dependent dispersion stability of the vesicles was well described by the normal DLVO theory. This indicates that the repulsive double-layer force is a major factor in stabilizing the vesicle dispersion, while the main driving force of the vesicle aggregation is an attractive van der Waals force between the vesicle bilayers.

The cryoTEM observation showed that the vesicles ($\beta = 0.4$ and 1.0) were polydisperse unilamellar, in addition to some multilamellar vesicles. The sediment ($\beta = 0.6$) consisted of many aggregated multilamellar vesicles with liquidlike hydrocarbon chains. The aggregated multilamellar vesicles had thick shell structures, made of closely stacked bilayers. The electrostatic repulsion between the stacked bilayers is suppressed by the complete binding of counterions NphS$^-$, leading to the change from unilamellar vesicles to aggregated multilamellar vesicles.

The composition analysis of the sediment indicated that the aggregated vesicles consisted of a 1:1 complex between the nonionic and the cationic species with the counterion NphS$^-$, rather than the simple salt C14DMAO$^+$ NphS$^-$. It is most likely that the interaction responsible for the specific 1:1 complex formation is the hydrogen bonding between the cationic and the nonionic headgroups ($-N^+-OH\cdots O-N-$). It is suggested that vesicle formation in the C14DMAO·$^1/_2$HCl−NaNphS system can be attributed to the combined effect of the hydrogen bonding between the cationic and the nonionic headgroups and the strong counterion NphS$^-$ binding.

Acknowledgment. The authors thank Mr. Y. Ono for carrying out the chloride ion activity measurement. This work was supported, in part, by a Grant-in-Aid for Scientific Research (B) (No. 12440200) from The Ministry of Education, Culture, Sports, Science and Technology, Japan. This study was partially supported by an Industrial Technology Research Grant Program in 2002 from the New Energy and Industrial Technology Development Organization (NEDO) of Japan and the Kurata Foundation.

References and Notes

(1) Israelachvili, J. N.; Mitchel, D. J.; Ninham, B. W. *J. Chem. Soc., Faradey Trans. 2* **1976**, *72*, 1525. Evans, D. F.; Wennerstrom, H. *The Colloidal Domain*, 2nd ed.; Wiley−VCH: New York, 1999.

(2) Gravsholt, S. *J. Colloid Interface Sci.* **1976**, *57*, 575.

(3) Rehage, H.; Hoffmann, H. *Faraday Discuss. Chem. Soc.* **1983**, *76*, 363.

(4) (a) Shikata, T.; Hirata, H. *Langmuir* **1987**, *3*, 1081. (b) Shikata, T.; Hirata, H.; Kotaka, T. *Langmuir* **1989**, *5*, 398.

(5) Caver, M.; Smith, T. L.; Gee, J. C.; Delichere, A.; Caponetti, E.; Magid, L. *Langumuir* **1996**, *12*, 691.

(6) Soltero, J. F. A.; Puig, J. E.; Manero, O. *Langumuir* **1996**, *12*, 2654.

(7) Bunton, C. A.; Michael, J. M.; Hidalgo, J.; Sepulveda, L. *J. Am. Chem. Soc.* **1973**, *95*, 3262.

(8) Bhat, M.; Gaikar, V. G. *Langumuir* **1999**, *15*, 4740.

(9) Brown, W.; Johansson, K.; Almgren, M. *J. Phys. Chem.* **1989**, *93*, 5888.

(10) Cates, M. W.; Candau, S. J. *J. Phys.: Condens. Matter* **1990**, *2*, 6869.

(11) Mishra, B. K.; Samant, S. D.; Pradhan, P.; Mishra, S. B.; Manohar, C. *Langumuir* **1993**, *9*, 894.

(12) Salkar, R. A.; Hassan, P. A.; Samant, S. D.; Valaulikar, B. S.; Kumar, V. V.; Kern, F.; Candau, S. J.; Manohar, C. *Chem. Commun.* **1996**, 1223.

(13) Narayanan, J.; Manohar, C.; Kern, F.; Candau, S. J. *Langumuir* **1997**, *13*, 5235.

(14) Horbaschek, K.; Hoffmann, H.; Thunig, C. *J. Colloid Interface Sci.* **1998**, *206*, 439.

(15) (a) Kawasaki, H.; Fukuda, T.; Yamamoto, A.; Fukada, K.; Maeda, H. *Colloids Surf., A* **2000**, *169*, 117. (b) Miyahara, M.; Kawasaki, H.; Fukuda, T.; Ozaki, Y.; Maeda, H. *Colloids Surf., A* **2001**, *183*, 475.

(16) Kawasaki, H.; Ookuma, K.; Maeda, H. *J. Colloid Interface Sci.* **2002**, *252*, 419.

(17) Maeda, H.; Yamamoto, A.; Souda, M.; Kawasaki, H.; Hossain, K. S.; Nemoto, N.; Almgren, M. *J. Phys. Chem. B* **2001**, *105*, 5411.

(18) Maeda, H.; Kakehashi, R. *Adv. Colloid Interface Sci.* **2000**, *88*, 275.

(19) Kawasaki, H.; Syuto, M.; Maeda, H. *Langmuir* **2001**, *17*, 8210.

(20) Kawasaki, H.; Syuto, M.; Maeda, H. *Chem. Lett.* **2000**, 972.

(21) Kawasaki, H.; Souda, S.; Tanaka, S.; Nemoto, N.; Karlsson, G.; Almgren, M.; Maeda. H. *J. Phys. Chem B* **2002**, *106*, 1524.

(22) Goddard, E. D.; Kung, H. C. *J. Colloid Interface Sci.* **1973**, *175*, 497.

(23) Ikeda, S.; Tsunoda, M.; Maeda, H. *J. Colloid Interface Sci.* **1979**, *70*, 448.

(24) Warr, G. G.; Grieser, F.; Evans, D. F. *J. Chem. Soc., Faraday Trans. 1* **1986**, *82*, 1829.

(25) Maeda, H. *Colloids Surf., A* **1996**, *109*, 263.

(26) Kawasaki, H.; Maeda, H. *Langmuir* **2001**, *17*, 2279.

(27) Kawasaki, H.; Imahayashi, R.; Maeda, H. *Langmuir* **2002**, *18*, 8358.

(28) Oka, K.; Otani, W.; Kameyama, K.; Kidai, M.; Takagi, T. *Appl. Theor. Electrophor.* **1990**, *1*, 273.

(29) Koppel, D. E. *J. Chem. Phys.* **1972**, *57*, 4814.

(30) Harris, J. K.; Rose, G. D.; Bruening, M. L. *Langmuir* **2002**, *18*, 5337.

(31) Verwey, E. J.; Overbeek, J. Th. G. *Theory of Stability of Lyophobic Colloids*; Elsevier: Amsterdam, 1948.

(32) Baba, T.; Zheng, L.-Q.; Minamikawa, H.; Hato, M. *J. Colloid Interface Sci.* **2000**, *223*, 235.

(33) Hogg, R.; Healy, T. W.; Fuerstenau, D. W. *Trans. Faraday Soc.* **1966**, *62*, 1638.

(34) Wiese, G.; Healy, T. W. *Trans. Faraday Soc.* **1970**, *66*, 490.

(35) Void, M. J. *J. Colloid Interface Sci.* **1961**, *16*, 1.

(36) Osmond, D. W. J.; Vincent, B.; Waite, F. A. *J. Colloid Interface Sci.* **1973**, *42*, 262.

(37) It was assumed that the bilayer thickness is equal to twice the length of a C14DMAO surfactant. The length of a C14DMAO surfactant, l_s, was assumed to consist of the hydrocarbon chain length, l_c, and the size of the headgroup a_0 (i.e. $l_s = l_c + a_0$). The l_c was estimated from the length for a flexible chain: $l_c = 0.75(0.15 + 0.127n)$. n is the total number of carbon atoms. The $N-CH_3$ distance in the amine headgroups was used as the a_0 ($a_0 = 0.36$ nm).

(38) Herder, C. E.; Claesson, P. M.; Herder, P. C. *J. Chem. Soc., Faraday Trans. 1* **1989**, *85*, 1933.

(39) Nakashima, T.; Shigematsu, M.; Ishibashi, Y.; Sugihara, G.; Inoue, T. *J. Colloid Interface Sci.* **1990**, *136*, 447.

(40) Walker, S. A.; Zasadzinski, J. A. *Langmuir* **1997**, *13*, 5076.

(41) Jung, H. T.; Coldren, B.; Zasadzinski, J. A.; Iampietri, D. J.; Kaler, E. W. *Proc. Natl. Acad. Sci.* **2001**, *98*, 1353.

(42) (a) Winterhalter, M.; Helfrich, W. *J. Phys. Chem.* **1988**, *92*, 6865. (b) Porte, G.; Ligoure, C. *J. Chem. Phys.* **1995**, *102* (10), 4290.

(43) Safinya, C. R.; Sirota, E. B.; Roux, D.; Smith, G. S. *Phys. Rev. Lett.* **1989**, *62*, 1134.

(44) Hassan, P. A.; Narayanan, J.; Menon, S. V. G.; Salkar, R. A.; Samant, S. D.; Manhar, C. *Colloids Surf., A* **1996**, *117*, 89.